한국광물학회지 제 20 권 제 2 호 (2007년 6월)
J. Miner. Soc. Korea, 20(2), 115-124 (June, 2007)

Gold Mineralization of the Youngbogari Mine, Youngdong Area

영동지역 영보가리 광산의 금광화 작용

Chul-Ho Heo (허 철 호)* · Se-Jung Chi (지 세 정)

Mineral Resources Group, Geology & Geoinformation Division, Korea Institute of Geoscience and Mineral Resources (KIGAM), 30 Gajeong-dong, Yuseong-gu, Daejeon 305-350, Korea
(대전광역시 유성구 가정동 30 한국지질자원연구원 지질기반정보연구부 광물자원연구실)

ABSTRACT : Electrum-sulfide mineralization of the Youngbogari mine area occurred in two stages of massive quartz veins that fill the fractures along the fault/shear zones in the Precambrian gneiss. Ore mineralogy is simple, consisting of arsenopyrite (31.4~33.4 atom.%As), pyrite, sphalerite (4.1~17.6 mole%FeS), galena, chalcopyrite, argentite, and electrum. Electrum (60.3~87.6 atom.%Ag) is associated with galena, chalcopyrite and late sphalerite infilling the fractures in quartz and sulfides. Fluid inclusion data show that ore mineralization was formed from H_2O-CO_2-CH_4-NaCl fluids ($X_{CO2+CH4}$ = 0.0 to 0.2) with low salinities (0 to 10 wt.% eq. NaCl) at temperatures between 200° and 370℃. Gold-silver mineralization occurred later than the base-metal sulfide deposition, at temperatures near 250℃ and was probably a result of cooling and decreasing sulfur fugacity caused by sulfide precipitation and/or H_2S loss through fluid unmixing.

Key words : electrum, fluid inclusion, unmixing

요약 : 충북 영동지역 영보가리 광산의 에렉트럼(은함량 = 60.3~87.6 atom.%)-황화광물 광화작용은 선캠브리아기 편마암 내의 단층열극을 충진한 석영맥으로 산출된다. 석영맥은 광물조성이 단순한 괴상이며, 구조적으로 2회에 걸쳐 형성되었다. 산출 광석광물은 비교적 단순하며, 유비철석(비소함량= 31.4~33.4 atom.%), 황철석, 섬아연석(철함량 = 4.1~17.6 mole% FeS), 방연석, 황동석, 휘은석 및 에렉트럼 등으로 구성된다. 유체포유물연구에 의하면, 광화작용은 CO_2+CH_4 함량($X_{CO2+CH4}$ = 0.0~0.2)과 저염도(0~10 wt.% NaCl 상당염농도)를 갖는 H_2O-CO_2-CH_4-NaCl계 유체로부터 200°~370℃의 온도범위에서 진행되었다. 금-은침전은 천금속계 황화광물 보다는 후기, 약 250℃ 근처에서 진행되었고, 유체불혼화에 따라 황화광물 침전 및 H_2S 일탈이 야기되면서 주로 냉각 및 유황분압의 감소에 기인하였다.

주요어 : 에렉트럼, 유체포유물, 불혼화

*Corresponding Author(교신저자): chheo@kigam.re.kr

INTRODUCTION

Most gold-silver vein deposits in Korea are intimately associated with Jurassic and Cretaceous granitic activities (Shimazaki *et al.*, 1986). Three main types of deposits have been previously documented which display a consistent relationship among depth, water-to-rock ratio, and Au/Ag ratio: Mesothermal-type gold deposits (So *et al.*, 1995; So and Yun, 1997; Heo *et al.*, 2003), Korean-type gold deposits (Shelton *et al.*, 1988), and silver-rich epithermal deposits (So *et al.*, 1994). Mesothermal-type gold deposits (So *et al.*, 1995; So and Yun, 1997; Heo *et al.*, 2003) have been scarcely reported in Korea. Therefore, a little is known about their ore genesis and ore fluid characteristics.

The Youngdong mining district, one of the most important gold-silver producers in Korea, contains several vein-type gold-silver deposits such as metamorphic-hosted gold-rich deposits, granite-hosted gold-silver deposits, and volcanic-hosted silver-rich deposits. The metamorphic-hosted gold- rich deposits are thought to correspond to the mesothermal-type deposits (So *et al.*, 1995; So and Yun, 1997; Heo *et al.*, 2003), however, there have been a few detailed studies on the fluid inclusion characteristics. The Youngbogari mine is a typical example of metamorphic-hosted gold-silver deposits. They had been in operation since 1936 but is now closed. Ore grades have 0.7 to 30 g/ton Au; 20 to 204 g/ton Ag. Ore reserves were estimated to be 145,200 metric tons.

In this paper, we describe the nature of ore mineralization at Younbogari mine and document the chemistry and origin of its mesothermal gold-depositing fluids.

GEOLOGIC SETTING and ORE VEINS

The Youngdong mining district, which is concentrating on twenty gold-silver deposits, is located approximately 170 km southeast of Seoul. Numerous hydrothermal quartz veins crosscut the Precambrian basement rocks in the central region of the Sobaegsan Massif.

The Precambrian basement rocks, occupying most of the mining area, consist of three major rock types: mica schist, biotite-banded gneiss, and granitic gneiss. Mica schist occurs as two small lenses within the gneiss complex, consisting of fine-grained quartz, feldspar, biotite, epidote, and chlorite. Biotite banded gneiss is the most abundant metamorphic rock in the study area. It is composed of quartz, plagioclase, biotite, muscovite, orthoclase and minor accessories such as chlorite, carbonates, sillimanite, cordierite, garnet and opaques, locally changing into the migmatitic gneiss, possibly by the injection of the granitic material. Coarse-grained granitic gneiss occurs in the study area, and shows ambiguous contacts with the biotite-banded gneiss due to strong migmatitization. It is characterized by the presence of microcline porphyroblasts, and is mainly composed of quartz, microcline, plagioclase, orthoclase, and biotite. Choo and Kim (1985) have obtained a whole-rock Rb-Sr date of 1,810 ± 10 Ma for the granite gneiss. The gneissosity of the metamorphic rocks in the study area has a general orientation of N18°～68°E strike with 70°～80°SE.

Late Jurassic granodiorite which contains quartz, plagioclase, orthoclase, microcline, biotite and accessory hornblende, zircon and sphene intrudes the gneiss complex at the eastern part of the mining area. A late Jurassic granodiorite yielded a K-Ar date of 146 Ma (sericite), regionally intrudes the metarmorphic rocks at the 6 km northeastern part of the study area. The contacts between the granite and the metamorphic rocks are highly migmatized, indicating that a migmatitization took place during the Jurassic granodiorite at 4～10 km southeastern part of the study area.

Early Cretaceous Baegmasan and Myeongryundong Formations in the northwestern part of the study area belong to the Youngdong group. Baegmasan Formation is composed wholly of greenish sandstone with minor intercalations of black shale. The strike and dip of strata are

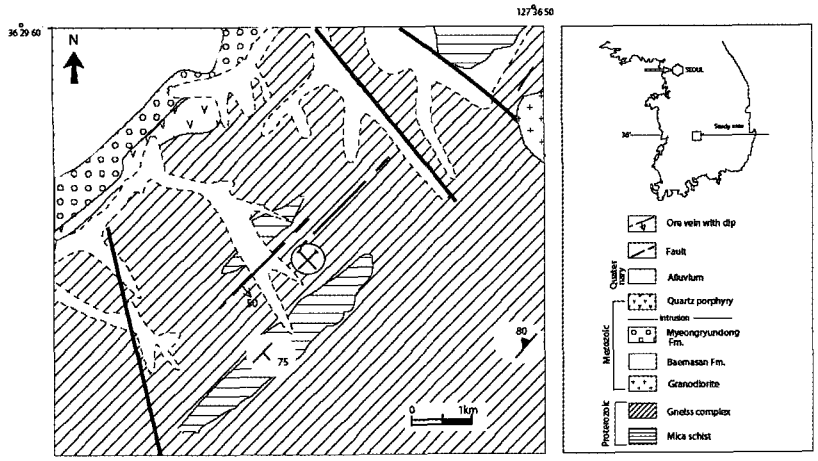

Fig. 1. Geologic map of the Youngbogari mine.

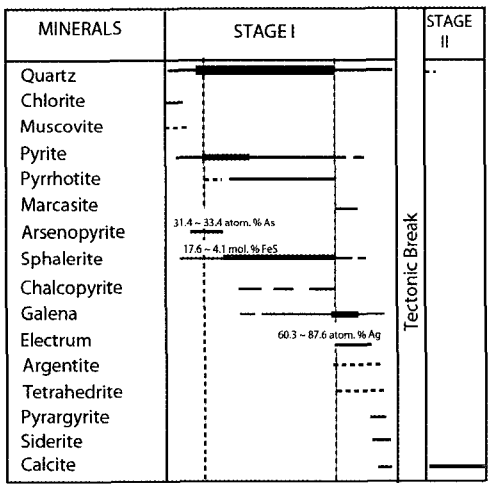

Fig. 2. Generalized paragenetic sequence of minerals from veins of the Youngbogari mine.

N30°~45°E and 15~20°SE, respectively. The Myeongryundong Formation, uppermost unit of Youngdong group, is composed of purple conglomerate and sandstone with intercalation of shale. Strike and dip are N30°~50°E and 40° SE.

Early Cretaceous quartz porphyry (K-Ar, 132 Ma for sericite) occurs along a northeastern direction parallel to the basin-forming fault and intrudes the Myeongryundong Formation (Fig. 1).

The two quartz veins of Youngbogari mine run up to 20~40 m along strike. Strike and dip directions are N20°~68°E and 70°~80°SE and vary considerably in width from 0.6 to 1 m. Weak alteration that have not carried economic gold values occurs in wall-rock gneiss, and some graphites occur along the mineralized fault plane. Available age data and geologic setting indicate that ore mineralization occurred in association with granitoids during the Jurassic activity (around 146 Ma). Ore mineralization occurs in one stage of quartz veins. The quartz veins are massive in appearance, but infrequently show small vugs and barren calcite veins crosscut the quartz veins. The ore mineralogy of the Youngbogari quartz veins is mainly simple, consisting of iron-rich base-metal sulfides, and electrum. The veins display a base-metal sulfide sequence, from vein margins to centers, of arsenopyrite + pyrite + sphalerite to a minor pyyrhotite + sphalerite + pyrite, and sphalerite + chalcopyrite + galena + electrum.

MINERALOGY and PARAGENESIS

Veins of the Youngbogari Au-Ag mine were formed during two mineralization stages separated by a major tectonic fracturing event (Fig. 2): Stage I, an iron-rich quartz-sulfide-gold stage; and stage II, carbonate stage. Stage I involves varying degrees of weak wall-rock alteration,

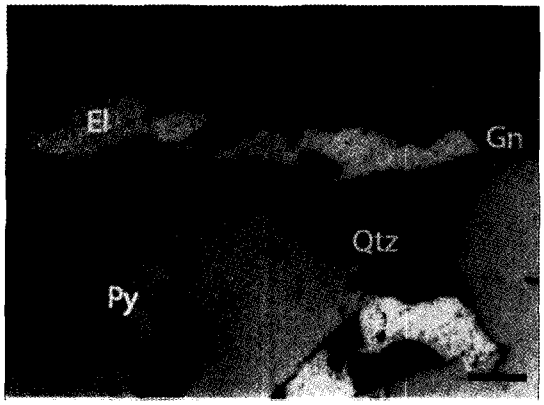

Fig. 3. Reflected light photomicrograph displaying the occurrence of electrum within galena, pyrite and sphalerite (stage I). Scale bar is 0.1 mm. Gold occurs within galena along the plane associated with quartz. Abbreviations: El = Electrum, Gn = Galena, Py = Pyrite, Qtz = Quartz.

bleaching the wall-rock gneiss.

Stage I

Economic quantities of gold and silver, together with quartz and sulfides, were introduced during this stage. Mineralogy and paragenesis of the Youngbogari mine are very similar to those of the Jurassic Samdong, Samhwanghak, Heungdeok and Daewon mines which are located about approximately 4～8 km southeast of the mine (So *et al.*, 1995; So and Yun, 1997). Compared to the mineralogy of the Korean Jurassic gold-silver deposits (Shelton *et al.*, 1988; So and Yun, 1997), the Youngbogari mine is characterized by the presence of gold-rich electrum.

Major alteration of wall rock occurred during stage I, extending up to a few meters from vein margins. Crudely zoned alteration envelopes are frequently present: an inner zone of sericitization and chloritization with pyrite and an outer zone of carbonatization characterized by the occurrence of muscovite. Chlorite is widely distributed in the wall rock near vein margins.

Stage I mineralization is characterized by dominant, massive gray to white quartz containing abundant sulfides. Massive quartz is frequently cut by randomly oriented sporadic fractures (mostly < 1 mm in width). These fractures are rehealed by later quartz, suggesting that some fracturing events were contemporaneous with the vein emplacement. Veins rarely occur along such fractures and are often filled with lesser amounts of euhedral clear quartz up to 7 mm (mostly < 1 mm), potassium feldspar and carbonates (siderite and ankerite).

Pyrrhotite occurs as anhedral masses intimately intergrown with sphalerite and chalcopyrite. It also occurs as rare inclusions intimately intergrown with chalcopyrite within sphalerite.

Pyrite occurs as fine euhedral to subhedral grains within quartz matrix and is a product of wall-rock alteration. Fine-grained pyrite aggregates occur with tiny euhedral arsenopyrites as mineralic bands at the vein margins, and contain rare anhedral pyrrhotite grains.

Arsenopyrites (31.4～33.4 atom.%As) which is the predominat sulfide found in the stage I veins, occurs as large euhedral to subhedral aggregates (up to 3 mm) throughout the veins and pyrite in mineralic bands along the vein margins. Cataclastic arsenopyrite is rehealed with quartz and base-metal sulfides, and electrum.

Sphalerite occurs throughout the veins and fine to medium grained sphalerite is rarely impregnated into the sericitized wall rock adjacent to the vein margins, as dispersed euhedral to subhedral grains. Sphalerite usually occurs as anhedral masses throughout the veins and is closely intergrown with pyrrhotite, chalcopyrite, galena and some pyrite. Lesser amounts of sphalerite occur within the microfractures cutting quartz and base-metal sulfides, and it is associated with late quartz, galena, chalcopyrite, electrum and argentite. Sphalerite (17.6～4.1 mole% FeS) compositions show a systematic variation, in accordance with their coexisting ore mineral assemblages.

Electrum (60.3～87.6 atom.%Ag) is frequently associated within galena, chalcopyrite and late sphalerite infilling the fractures in quartz and sulfides (Fig. 3).

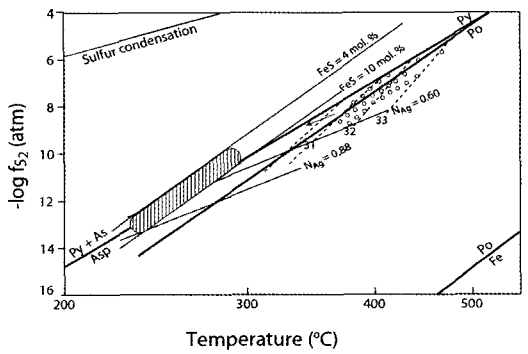

Fig. 4. Sulfur fugacity versus temperature diagram showing the ranges of ore depositional conditions indicated by electrum-sphalerite-pyrite-argentite assemblages from the Youngbogari mine. Hatched area represents the conditions of gold deposition in stage I (Barton and Toulmin, 1964; Kretchmar and Scott, 1976; Barton and Skinner, 1979). Abbreviations: Py = pyrite, As = Arsenic, Asp = Arsenopyrite, Po = Pyrrhotite, N_{Ag}= Atomic fraction of Ag in electrum, FeS = iron mole percent of sphalerite.

Stage II

Stage II represents the introduction of massive white calcite which fills open-spaces created by post-ore faulting and brecciation.

THERMOCHEMICAL IMPLICATIONS OF GOLD DEPOSITION

Due to the variation of depositional environments (eg., f_{S_2}, f_{O_2}, pH, etc), gold content of electrum varies (Barton and Toulmin, 1964; Shikazono, 1985). Electrum-sphalerite-pyrite-argentite assemblage is present in stage I veins of the Youngbogari mine. Considering that the sphalerite (mole% FeS = 4 to 10) and electrum (atomic fraction of Ag = 0.60 to 0.88) were in equilibrium, temperature and sulfur fugacity of gold depositing fluids can be estimated from phase relations in the system Fe-Zn-S (Scott and Barnes, 1971) and Au-Ag (Barton and Toulmin, 1964). Gold deposition at Younbogari occurred at temperatures of about 250° to 300℃, corresponding to fugacities of sulfur (log f_{S_2}) at about -11 to -14 atm (Fig. 4).

FLUID INCLUSION STUDIES

About 50 vein quartz samples for fluid inclusion study were collected from underground ore stopes and from the surface area. Additional some calcite samples were obtained from the postore carbonate vein. Sphalerites were not suitable to study the fluid inclusions because of their opacity due to the high contents of iron. Data were obtained on a FLUID Inc. gas flow heating-freezing stage calibrated with pure CO_2, H_2O (synthetic inclusions), and various kinds of organic solvents (Hollister *et al.*, 1981). Heating rates varied widely but were maintained near 1 ℃/min for determination of melting temperatures and carbonaceous phase homogenization temperatures, and about 10℃/min for determination of total homogenization temperatures. On the measurements of melting points, repeated cycling techniques were used over the expected temperatures. Temperatures of total homogenization, and of melting (of carbonaceous phase, ice, and clathrate) and carbonaceous phase homogenization have standard errors of ±0.1 and ±0.2℃, respectively. In addition to microthermometric measurements, the mole fraction of each phase was visually determined on selected inclusions.

Occurrence and Compositional Types of Fluid Inclusions

Massive gray to white quartz was inclusion-laden, probably due to repeated fracturing and healing, both during and after quartz deposition. The size of fluid inclusions ranged from < 3 to 25 μm. Three main types of fluid inclusions were identified based on their appearance at room temperature, combined with their cooling behavior (down to about -15℃) and slight heating (up to about 25℃). By order of de-

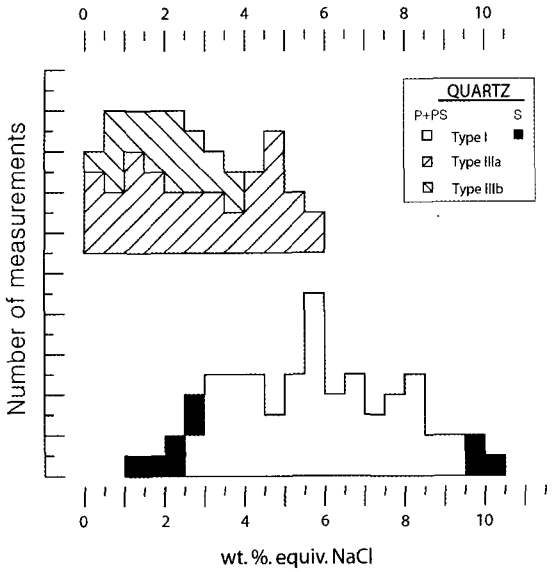

Fig. 5. Frequency diagram of salinities of fluid inclusions in stage I vein quartz of the Youngbogari mine. Abbreviations: P + PS = primary and pseudosecondary, S = secondary.

creasing abundance, they are : type I (liquid-rich), type III (dominantly H_2O-CO_2 type), and type II (vapor-rich type).

Type I inclusions are generally simple or tabular in shape or are negative crystals, and the volume of the gas bubble comprises 10 to 45 percent of the total inclusion. Some of the type I inclusions indicate the presence of minor amounts of CO_2.

Type II inclusions, having a gas bubble of more than 40 vol.% (mostly > 50%) at room temperature, are usually irregular in shape and occasionally show the necking-down phenomena. Type II occurs as small amounts along the planes crosscutting quartz grains, suggesting their secondary origin. They occur as both primary and secondary inclusions, and do not contain CO_2 and are interpreted to be simple H_2O-salt inclusion.

Type III fluid inclusions were classified into two subtypes according to their relative abundance of carbonaceous phases at 20℃: type IIIa (H_2O > CO_2) and type IIIb (CO_2 > H_2O). Their volumetric proportions of carbonaceous phases (liquid + vapor) at 20℃ are: type IIIa inclusions, from about 10 to 35 percent, with a significant number in the range of 15 to 20 percent; type IIIb inclusions, from about 65 to 90 percent. The whole range of carbonaceous phase volumetric proportions usually has been observed within individual samples, which is a result of fluid unmixing. However, some inclusions containing a relatively constant phase ratio ranging from 20 to 25 vol.% of carbonaceous phase sometimes form an inclusion cluster, suggesting an entrapment of a homogeneous fluid. Low-temperature inclusion behavior indicates the presence of CH_4.

It is impossible to establish a consistent fluid inclusion chronology because repeated fracturing and healing both during and after quartz deposition frequently prevent distinguishing among primary and secondary inclusions using normal criteria (Roedder, 1984). This inherent difficulty of clarity has shown in crack-healing experiments with quartz (Sterner and Bodnar, 1984). Therefore, we have employed a more practical distinction in this study between primary + psuedosecondary inclusions and obvious secondary inclusions.

Heating and Freezing Data

About 360 fluid inclusions (296 primary + psuedosecondary and 44 secondary inclusions in stage I vein quartz; 13 primary + psuedosecondary and 3 secondary inclusions in stage II calcite) were examined. Salinity data were reported based on freezing point depression in the system H_2O-NaCl (Potter *et al.*, 1978) for liquid-rich aqueous inclusions, and on clathrate melting temperatures for CO_2-bearing inclusions (Collins, 1979).

Primary + pseudosecondary and secondary inclusions in stage I gray to white quartz include type I, type II and type III inclusions. The wide range of homogenization temperatures of fluid inclusions in vein quartz probably reflects several hydrothermal episodes rather than one spe-

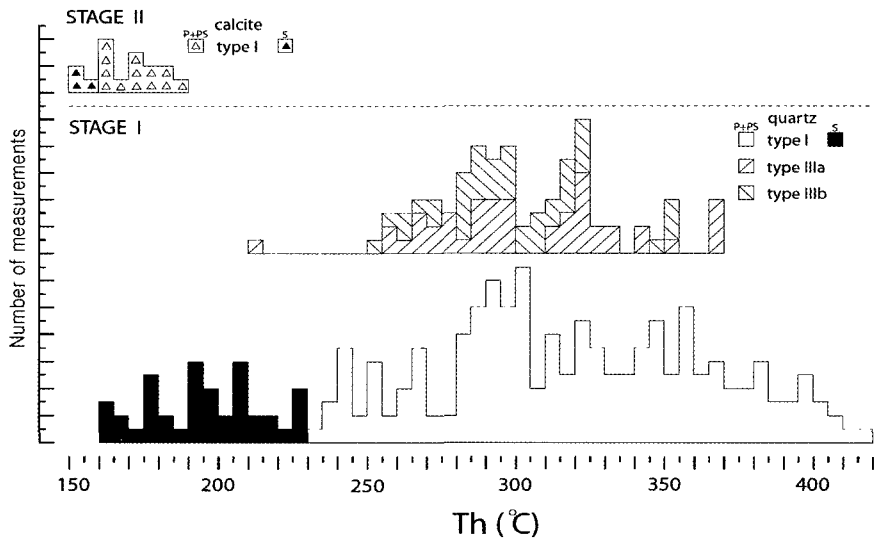

Fig. 6. Frequency diagrams of homogenization temperatures of fluid inclusions in stage I and II (minerals) from the Youngbogari mine. Symbols are the same as in Fig. 5.

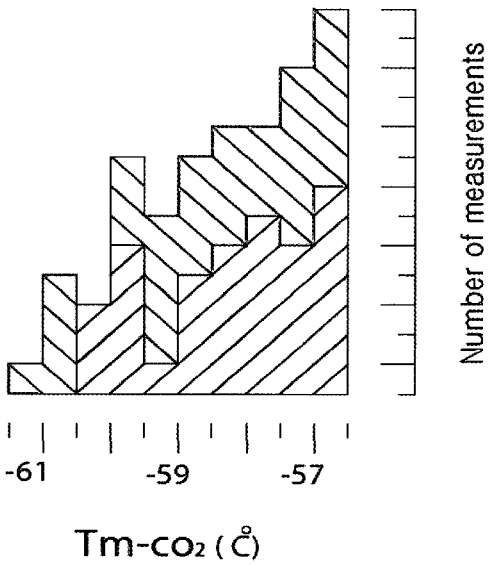

Fig. 7. Frequency diagram of Tm_{CO2} homogenization temperatures for type IIIa and IIIb fluid inclusions in the Youngbogari mine. Symbols are the same as in Fig. 5.

cific event, as indicated by textural evidence of multiple opening and filling of the veins.

Type I inclusions in stage I veins

The first ice melting of type I inclusions, although it was so difficult to observe that only a few measurements were recorded, recognized at near -21℃. The measured temperatures indicate the predominance of NaCl among dissolved salts (Crawford, 1981). Final ice melting temperature in primary + pseudosecondary type I inclusions had the range of -1.6 to -6.1℃ corresponding to the salinities of 2.7 to 9.3 wt. % NaCl (Fig. 5). Primary + pseudosecondary type I inclusions homogenized totally to liquid phase at temperatures of 232° to 418℃ (Fig. 6). Final ice melting temperature in the secondary type I inclusions had the range of -0.7 to -6.9℃ corresponding to the salinities of 1.2 to 10.4 wt. % NaCl. They homogenized at clearly lower temperatures in the range of 163° to 228℃ (Figs. 5 and 6).

Type IIIa inclusions in stage I veins:

Type IIIa inclusions have CO_2 melting temperatures of -60.4 to -56.6℃ (Fig. 7), suggesting the presence of CH_4 (Burruss, 1981). Homogenization temperatures of the CO_2 phase (Th_{CO2}: to liquid phase) are 19.2° to 29.6℃ (Fig. 8). Homogenization temperatures of carbonaceous phase are variable within single sam-

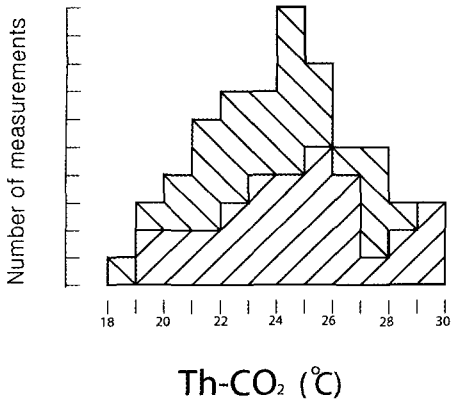

Fig. 8. Frequency diagram of homogenization temperatures of Th_{CO2} for type IIIa and IIIb fluid inclusions in the Youngbogari mine. Symbols are the same as in Figure 5.

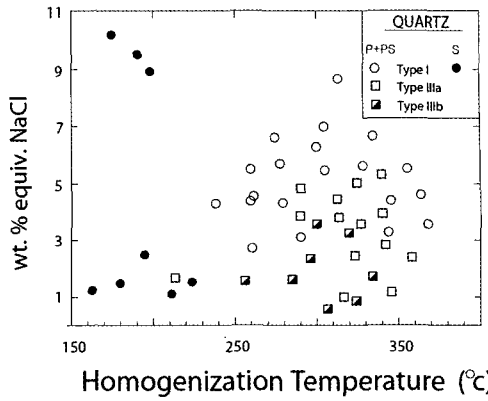

Fig. 9. Total homogenization temperature versus salinity diagram for fluid inclusions in stage I vein quartz of the Youngbogari mine.

ples, suggesting that the density of carbonaceous phase was highly variable at the time of entrapment, possibly due to pressure fluctuations. No further phase changes could be observed on heating. Tm-clathrate tempertures of type IIIa inclusions have the ranges of 5.3 to 11.3℃ corresponding to salinities of 0.4 to 5.8 wt.% eq. NaCl (Fig. 5).

Type IIIb inclusions in stage I veins:

Type IIIb inclusions have CO_2 melting temperatures (Tm_{CO2}) ranges -61.4 to -56.6°C (Fig. 7). Homogenization temperatures of the CO_2 phase (Th_{CO2}: to liquid phase) are 18.3° to 28.4℃ (Fig. 8). Tm-clathrate tempertures of type IIIb inclusions have the ranges of 8.0 to 9.8℃ corresponding to salinities of 0.8 to 3.9 wt.% eq. NaCl (Fig. 5). Most type III inclusions examined generally decrepitated prior to total homogenization. Therefore, total homogenization temperatures of a small number of these inclusions were recorded. When the decrepitation occurred before anticipated homogenization, this temperature was used as a minimum homogenization temperature. Total homogenization temperatures of type IIIa and IIIb, including useful decrepitation temperatures, were 213°~367℃ (type IIIa) and 253°~353℃ (type IIIb), respectively (Fig. 6).

Type I inclusions in stage II veins:

Primary aqueous fluid inclusions in white calcites occurring in post-ore carbonate stage homogenized to liquid phase of 163°~188℃ (Fig. 6). Homogenization temperatures of obvious secondary inclusions were in the range of 151° to 158℃ (Fig. 6).

Relationship of Fluid Inclusions to Gold Mineralization

As described in "Mineralogy and Paragenesis" section, electrum grains occur within the randomly oriented healed fractures. Such mineralization occurrence can be attributed to the hydrothermal fluids trapped as the pseudosecondary and/or secondary fluid inclusions in vein quartz. Some of the type III inclusions occur in the healed fractures which continue to be the gold-containing veinlets, suggesting their intimate linkage with gold mineralization.

As described earlier, such primary type III inclusions homogenized totally at temperatures of 260° to 350℃ (avg. = 289℃). These temperatures are in good agreement with the estimated temperatures using ore mineral assemblage and mineral compositional data (Fig. 4). Therefore, these temperature ranges are thought to have been linked to the deposition temperatures of gold mineralization at the Youngbogari mine.

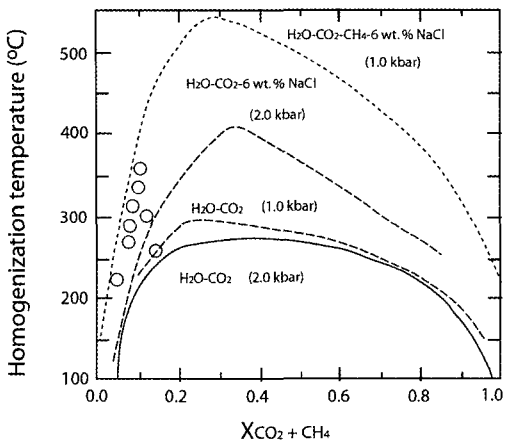

Fig. 10. Bulk composition ($X_{CO2+CH4}$) versus total homogenization temperature diagram for type III inclusions, showing topological relationships between estimated T-X data and solvi for the system for H_2O-CO_2-CH_4-NaCl systems at different pressure and salinity conditions (Bowers and Helgeson, 1983).

The relationship between temperature and salinity of stage I fluids suggests a history of fluid unmixing produced by progressive cooling and/or pressure decrease over the temperature range of 260° to 350℃ (Fig. 9). Carbonaceous type III inclusions display a trend of decreasing salinity (from ~5 to 0 wt.% eq. NaCl) with decreasing temperature, whereas aqueous type I inclusion display a reverse trend of increasing salinity (up to ~9 wt.% eq. NaCl). Bowers and Helgeson (1983) have shown that unmixing of a relatively low-salinity H_2O-CO_2 fluid can produce a high-salinity H_2O-rich fluid, because nearly all of the salt will fractionate into the H_2O-rich liquid phase rather than into the CO_2-rich vapor phase. These observations indicate that the type III fluid inclusions represent the trapping of immiscible H_2O-CO_2 fluids which evolved through CO_2 effervescence.

Pressure Considerations

As described above, the primary and pseudosecondary inclusions in vein quartz are thought to represent trapping of coexisting fluids during unmixing (CO_2 effervescence). In such case, formation pressures of fluid inclusions can be calculated, although it is a delicate matter to obtain pressure and temperature conditions from trapped immiscible aqueous and carbonaceous fluids. In such cases, the homogenization temperature of coexisting H_2O-rich and CO_2-rich inclusions generally corresponds to the entrapment temperature of these fluids.

As shown in Fig. 10, most inclusion compositions of the Youngbogari mine fall in the range between the H_2O-CO_2-6 wt.% NaCl (2 kbar) and the H_2O-CO_2-CH_4-6 wt.% NaCl (1 kbar) solvus. Their intersecting temperatures are about 210° to 370℃, which are in the range of the type I and III homogenization temperatures. This range of pressures corresponds to minimum depths of unmixing of about 5 to 8 km, assuming lithostatic conditions.

SUMMARY

1) Gold mineralization of the Youngbogari mine occurred in two stages of massive quartz veins that fill the fractures along the fault/shear zones in the Precambrian gneiss within the central region of the Sobaegsan Massif.

2) Ore mineralogy is relatively simple, consisting of arsenopyrite, pyrite, sphalerite, galena, chalcopyrite, argentite, and electrum. Electrum (60.3~87.6 atom.%Ag) is closely associated with galena, chalcopyrite and late sphalerite infilling the fractures in quartz and sulfides.

3) Fluid inclusion data show that auriferous mineralization was formed from H_2O-CO_2-CH_4-NaCl fluids with low salinities at temperatures between 200° and 370℃.

4) From the mineral paragenesis and fluid inclusion study, it is suggested that gold-silver mineralization occurred later than the base-metal sulfide deposition, at temperatures near 250℃ and was probably a result of cooling and decreasing sulfur fugacity caused by sulfide precipitation and/or H_2S loss through fluid unmixing.

ACKNOWLEDGEMENTS

This study was financially supported by the KIGAM fund (07-3111) titled as "Revaluation of strategy mineral resources and development of exploration techniques for ore deposits".

REFERENCES

Barton, P.B., Jr. and Toulmin, P. III. (1964) The electrum-tarnish method for the determination of the fugacity of sulfur in laboratory sulfide system. Geochimica et Cosmochimica Acta, 28, 619-640.

Barton, P.B., Jr. and Skinner, B. J. (1979) Sulfide mineral stabilities: In. Barnes, H.L., ed. Geochemistry of hydrothermal ore deposits, New York, Wiley, 278-403.

Bowers, T. S. and Helgeson, H. C. (1983) Calculation of thermodynamic and geochemical consequences of nonideal mixing in the system H_2O-CO_2-NaCl on phase relations in geologic systems: Equation of state for H_2O-CO_2-NaCl fluids at high pressures and temperatures. Geochimica et Cosmochimica Acta, 47, 1247-1275.

Burruss, R.C. (1981) Analysis of fluid inclusions : Phase equilibria at constant volume. American Journal of Science, 281, 1104-1126.

Choo, S. H. and Kim, S. J. (1985) A study of Rb-Sr age determinations on the Ryeongnam Massif (I): Pyeonghae, Buncheon and Kimcheon granitic gneisses. Annual Report 85-24, Korea Institute Energy and Resources, 7-39.

Collins, P.L.F. (1979) Gas hydrates in CO_2-bearing fluid inclusion and the use of freezing data for estimation of salinity. Economic Geology, 74, 1435-1444.

Crawford, M.L. (1981) Phase equilibria in aqueous fluid inclusions. Mineralogical Association Canada Short Course Handbook, 6, 75-100.

Heo, C. H., Yun, S.T. and So, C. S. (2003) Sulfur isotope characteristics of mesothermal-type gold deposits in the Boseng-Jangheung area, Korea. Neues Jahrbuch fur Mineralogie Abhandlungen, 178, 107-129.

Hollister, L.S., Crawford, M.L., Roedder, E., Burruss, R.C., Spooner, E.T.C. and Touret, J. (1981) Practical aspects of microthermometry. Mineralogical Association of Canada Short Course Handbook, 6, 278-301.

Kretschmar, U. and Scott, S.D. (1976) Phase relations involving arsenopyrite in the system Fe-As-S and their application. Canadian Mineralogist, 14, 364-386.

Potter, R.W. III., Clynne, M.A. and Brown, D.L. (1978) Freezing point depression of aqueous sodium chloride solutions. Economic Geology, 73, 284-285.

Roedder, E. (1984) Fluid inclusions. Reviews in Mineralogy, 12, 644p.

Scott, S.D. and Barnes, H.L. (1971) Sphalerite geothermometry and geobarometry. Economic Geology, 66, 653-669.

Shelton, K.L., So, C.S. and Chang, J.S. (1988) Gold-rich mesothermal vein deposits of the Republic of Korea: Geochemical studies of the Jungwon gold area. Economic Geology, 83, 1221-1237.

Shikazono, N. (1985) A comparison of temperatures estimated from electrum-sphalerite-pyrite-argentite assemblage and filling temperature of fluid inclusions from epithermal Au-Ag vein deposits in Japan. Economic Geology, 80, 1415-1424.

Shimazaki, H., Lee, M.S., Tsusue, A. and Kaneda, H. (1986) Three epochs of gold mineralization in South Korea. Mining Geology, 36, 265-272.

So, C.S., Yun, S.T., Youm, S.J. and Heo, C.H. (1994) Fluid inclusion and stable isotope studies of gold- and silver-bearing vein deposits, South Korea: Silver-rich epithermal mineralization of the Keumryeong mine. Neues Jahrbuch fur Mineralogie Abhandlungen, 167, 57-88.

So, C.S., Yun, S.T. and Shelton, K.L. (1995) Mesothermal gold vein mineralization of the Samdong mine, Youngdong mining district, Republic of Korea. Mineralium Deposita, 30, 384-396.

So, C.S. and Yun, S.T. (1997) Jurassic mesothermal gold mineralization of the Samhwanghak mine, Youngdong area, Republic of Korea: Constraints on hydrothermal fluid chemistry. Economic Geology, 92, 60-80.

Sterner, S.M. and Bodnar, R.J. (1984) Synthetic fluid inclusions in natural quartz I. Compositional types synthesized and applications to experimental geochemistry. Geochimica et Cosmochimica Acta, 48, 2659-2668.

2007년 4월 6일 원고접수, 2007년 6월 20일 게재승인.